Journal of Applied Mechanics Vol.13, pp.877-882 (August 2010) JSCE

Stability Analysis of Fluvial Bars Using a New Bed Load Formula

新しい掃流砂量公式を用いた砂州の安定解析

Adichai PORNPROMMIN* and Norihiro IZUMI**
ポンプロミン アディチャイ・泉 典洋

*Member, D.Eng., Assistant Professor, Dept. Water Resources Engineering, Kasetsart University
(50 Phaholyothin Rd., Jatujak, Bangkok 10900, Thailand)
**Member, PhD, Professor, Div. Field Engineering for the Environment, Hokkaido University
(North 13 West 8, Kitaku, Sapporo 060–8628, Japan)

Recent research shows that the Bagnold's hypothesis breaks down when applied to equilibrium bed load transport on beds with transverse slopes above a relatively modest value that is well below the angle of repose. Since fluvial bar formation is strongly influenced by the transverse slopes, the results of our previous study, using the bed load formula based on Bagnold's hypothesis, become questionable. Thus, in this study, we reanalyze our previous study using the linearized version of the new bed load formula based on the entrainment function. It is found that the new bedload formula gives better agreements on bar length and bar celerity with extensive experimental data than the bed load formula used in the previous study. However, bar celerity is still overestimated. It is hypothesized that the linearized version of the new bed load formula is not sufficient to simulate the bar celerity due to the steep transverse slopes of fluvial bars.

Key Words : *bar formation, nonlinear analysis, amplitude expansion method, bed load formula*

1. Introduction

Fluvial bar formation has been one of the most fruitful research topics for geomorphologists and river engineers. It has been known for decades that fluvial bar formation is generated by the instability between water flow and movable beds. At present, many researchers investigated fluvial bar formation in terms of nonlinear stability analysis[1)−6)]. In their analyses, only bed load is considered. Thus, the accuracy of their results depends on the accuracy of bed load formula used in their analyses.

Recently, Seminara *et al.*[7)] have scrutinized the Bagnold's hypothesis and found that the hypothesis breaks down when applied to equilibrium bed load transport on beds with transverse slopes above a relatively modest value that is well below the angle of repose. Then, a new bed load formula has been proposed by Parker *et al.*[8)]. Since bed load on fluvial bars is subject to a strong effect of the transverse slopes, the results of our previous analysis[5)] (with the use of the bed load formula by Kovacs and Parker[9)] based on the Bagnold's hypothesis) become uncertain. In this study, we reanalyze the bar stability problem using the new bed load formula[8)].

2. Formulation

2.1 Governing equations

Let us consider flow in a straight channel with a constant width $\tilde{W}$ and non-erodible banks (**Fig. 1**). The normalized St. Venant shallow water equations are expressed as[4)]

$$F^2\left(U\frac{\partial U}{\partial x}+V\frac{\partial U}{\partial y}\right)=-\frac{\partial H}{\partial x}-\frac{\partial Z}{\partial x}-\beta S\frac{(U^2+V^2)^{1/2}U}{(1+2.5C_{fn}^{1/2}\ln H)^2H} \quad (1)$$

$$F^2\left(U\frac{\partial V}{\partial x}+V\frac{\partial V}{\partial y}\right)=-\frac{\partial H}{\partial y}-\frac{\partial Z}{\partial y}-\beta S\frac{(U^2+V^2)^{1/2}V}{(1+2.5C_{fn}^{1/2}\ln H)^2H} \quad (2)$$

$$\frac{\partial UH}{\partial x}+\frac{\partial VH}{\partial y}=0 \quad (3)$$

$$S=\frac{C_{fn}U_n^2}{gH_n},\quad F=\frac{U_n}{(gH_n)^{1/2}},\quad \beta=\frac{W}{H_n} \quad (4a\text{–}c)$$

where x and y are the streamwise and lateral coordinates normalized by the width respectively, U and V

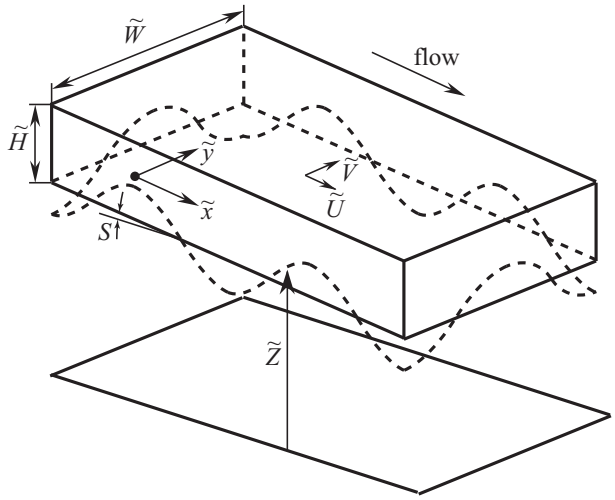

Fig. 1 Sketch of coordinate system.

are the velocity components in the x and y directions normalized by the base flow velocity respectively, H and Z are the flow depth and bed elevation normalized by the base flow depth respectively, S is the bed slope, F is the Froude number in the normal flow condition, β is the aspect ratio, and C_{fn}, U_n and H_n are the friction coefficient, streamwise velocity and flow depth in the normal flow condition, respectively.

The time variation of bed elevation can be described by the normalized Exner sediment continuity equation, that is

$$\frac{\partial Z}{\partial t} + \frac{\partial Q_{bx}}{\partial x} + \frac{\partial Q_{by}}{\partial y} = 0 \tag{5}$$

where t is time, and Q_{bx} and Q_{by} are the x and y components of the normalized total bed load transport rate.

For simplicity, the linearized version of the new bed load formula by Parker *et al.*[8] is used in this study. The normalized total bed load is

$$Q_b = \left[\frac{U^2+V^2}{(1+2.5C_{fn}^{1/2}\ln H)^2} - \Theta\right] \times \left[\frac{(U^2+V^2)^{1/2}}{1+2.5C_{fn}^{\frac{1}{2}}\ln H} - 0.7\Theta^{\frac{1}{2}}\right] \Big/ (1-\Theta)\left(1-0.7\Theta^{\frac{1}{2}}\right) \tag{6}$$

and the angle between the direction of the applied shear stress and the direction of particle velocity ψ can be described by

$$\tan\psi = \Gamma_0\sqrt{\frac{\Theta(1+2.5C_{fn}^{1/2}\ln H)^2}{U^2+V^2}}\tan\phi \tag{7}$$

where $\Theta = \tau_{co}/\tau_n$, τ_{co} is the critical Shields stress for a flat bed, and τ_n is the Shields stress in the normal flow condition, Γ_0 is a constant ($= 0.7$), and ϕ is the transverse bed angle to the direction of the applied shear stress. Thus,

$$\tan\phi = \left(-u\frac{\partial z}{\partial y} + v\frac{\partial z}{\partial x}\right) \Big/ \beta\sqrt{U^2+V^2} \tag{8}$$

Therefore, the x and y components of the normalized total bed load transport rate Q_{bx} and Q_{by} are

$$Q_{bx} = Q_b\cos(\theta+\psi) \tag{9}$$

$$Q_{by} = Q_b\sin(\theta+\psi) \tag{10}$$

where θ is the angle between the streamwise direction x and the direction of the applied shear stress. Thus,

$$\tan\theta = V/U \tag{11}$$

The following normalization has been used to derive the above equations:

$$(\tilde{x},\tilde{y}) = \tilde{W}(x,y), \quad \left(\tilde{U},\tilde{V}\right) = \tilde{U}_n(U,V) \tag{12a–d}$$

$$\left(\tilde{H},\tilde{Z},\tilde{D}_s\right) = \tilde{H}_n(H,Z,D_s), \quad \tilde{t} = \frac{(1-\lambda_p)\tilde{H}_n\tilde{W}}{\tilde{Q}_n}t \tag{12e–h}$$

$$\tilde{Q}_n = \left(R_s g\tilde{D}_s^3\right)^{1/2} K_1(\tau_n-\tau_{co})\left(\tau_n^{1/2}-0.7\tau_{co}^{1/2}\right) \tag{13}$$

where the tilde denotes the dimensional variables, $\tilde{Q}_n$ is the sediment transport rate in the normal flow condition, λ_p is the porosity, R_s is the submerged specific gravity, $\tilde{D}_s$ is the sediment diameter, and K_1 is a constant ($= 7.67$).

2.2 Asymptotic expansion

The following perturbations are imposed to the normal flow:

$$(U,V,H,Z) = (1,0,1,-\beta Sx) + (U_1,V_1,H_1,Z_1) + (U_2,V_2,H_2,Z_2) + (U_3,V_3,H_3,Z_3) \tag{14a–d}$$

where the subscripts 1, 2 and 3 denote the first order terms at $O(A)$, the second order terms at $O(A^2, AA^*)$ and the third order terms at $O(A^3, A^2A^*)$, respectively, and * denotes the complex conjugate.

Assume that the fundamental disturbance is expressed by small perturbation with the bar mode m. The first order terms can be written as

$$(U_1,V_1,H_1,Z_1) = AE_1\Gamma_1(u_{111},v_{111},h_{111},z_{111}) + \text{c.c.} \tag{15}$$

where c.c. denotes the complex conjugate of the preceding term, and E_m and Γ_m are

$$E_m = \exp mikx, \quad \Gamma_m = \begin{cases} \cos m\pi y & \text{for} \quad U,H,Z \\ \sin m\pi y & \text{for} \quad V \end{cases} \tag{16a,b}$$

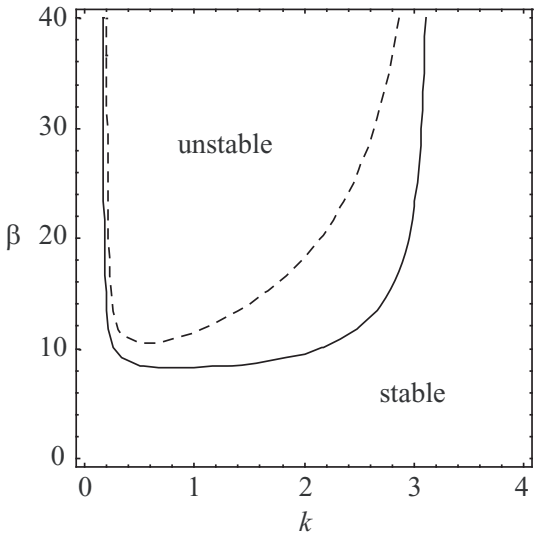

Fig. 2 Instability diagram. Lines denote the neutral curves, where the linear growth rate $\mathrm{Re}[\lambda_0]$ equals to zero. The solid line is the present result, and the dashed line is the previous result, where $m = 1$, $S = 0.005$, $F = 0.7$, and $\Theta = 0.5$.

where the origin of y is taken at the right side wall as shown in **Fig. 2**, and the cases $m = 1$ and $m > 1$ correspond to single and multiple bars, respectively.

The time development of the fundamental amplitude of the disturbance A can be described by the Landau equation in the form

$$\frac{\mathrm{d}A}{\mathrm{d}t} = \lambda_0 A + \lambda_1 A^2 A^* + \cdots \tag{17}$$

where λ_0 is the linear growth rate, and λ_1 is the Landau constant that characterize the nonlinear development of the disturbance. When the real part of the linear growth rate $\mathrm{Re}[\lambda_0] > 0$ and the real part of the Landau constant $\mathrm{Re}[\lambda_1] < 0$, the amplitude of the disturbance approaches the equilibrium amplitude A_e $(= \sqrt{-\mathrm{Re}[\lambda_0]/\mathrm{Re}[\lambda_1]})$ asymptotically (supercritical stability).

2.3 First order expansion

We have the following equations at the first order:

$$F^2\frac{\partial U_1}{\partial x}+\frac{\partial H_1}{\partial x}+\frac{\partial Z_1}{\partial x}+2\beta S U_1-\beta S\left(1+5C_{fn}^{1/2}\right)H_1 = 0 \tag{18}$$

$$F^2\frac{\partial V_1}{\partial x}+\frac{\partial H_1}{\partial y}+\frac{\partial Z_1}{\partial y}+\beta S V_1 = 0 \tag{19}$$

$$\frac{\partial U_1}{\partial x}+\frac{\partial H_1}{\partial x}+\frac{\partial V_1}{\partial y} = 0 \tag{20}$$

$$\frac{\partial Z_1}{\partial t}+\theta_1\frac{\partial U_1}{\partial x}+\left(1-\Gamma_0 S\sqrt{\Theta}\right)\frac{\partial V_1}{\partial y} - \frac{5}{2}C_{fn}^{1/2}\theta_1\frac{\partial H_1}{\partial x}-\frac{\Gamma_0\sqrt{\Theta}}{\beta}\frac{\partial^2 Z_1}{\partial y^2} = 0 \tag{21}$$

where

$$\theta_1 = \frac{1}{1-0.7\sqrt{\Theta}}+\frac{2}{1-\Theta} \tag{22}$$

By substituting the first order perturbations (15), the above equations are rewritten in matrix forms

$$\mathbf{L}_{abc}\begin{bmatrix} u_{abc} \\ v_{abc} \\ h_{abc} \\ z_{abc} \end{bmatrix} = 0, \quad a=b=c=1 \tag{23}$$

where the subscript a denotes the order of expansion, the subscripts b and c denote terms accompanying E_b and Γ_c, respectively. The matrix $\mathbf{L}_{abc}$ can be written as

$$\mathbf{L}_{abc} = [l_{ij}], \quad i,j = 1,2,3,4 \tag{24a}$$

$$l_{11} = 2\beta S + \mathrm{i}bkF^2,\ l_{12} = 0,\ l_{13} = \mathrm{i}bk - \beta S\left(1+5C_{fn}^{\frac{1}{2}}\right)$$

$$l_{14} = \mathrm{i}bk,\ l_{21} = 0,\ l_{22} = \beta S + \mathrm{i}bkF^2,\ l_{23} = -cm\pi$$

$$l_{24} = -cm\pi,\ l_{31} = \mathrm{i}bk,\ l_{32} = cm\pi,\ l_{33} = \mathrm{i}bk,\ l_{34} = 0$$

$$l_{41} = \mathrm{i}bk\theta_1,\ l_{42} = cm\pi\left(1-\Gamma_0 S\sqrt{\Theta}\right),$$

$$l_{43} = -\frac{5}{2}\mathrm{i}bkC_{fn}^{1/2}\theta_1,\ l_{44} = \Lambda_{abc} + \frac{\Gamma_0\sqrt{\Theta}}{\beta}(cm\pi)^2 \tag{24b–q}$$

where

$$\Lambda_{111} = \lambda_0 \tag{24r}$$

Solving (23) with the solvability condition that the determinant of $\mathbf{L}_{1bc}$ must vanish for non-trivial solution, we can obtain the linear growth rate λ_0 as a function of the parameters m, β, S, F, Θ and k.

Due to the limitation of space, solving the second and third order expansion is omitted here. Please refer to our previous study[4] for solving the solutions.

3. Results and Discussion

(1) Instability diagram

In this study, the critical Shields stress τ_{co} is set to be 0.035 as the previous study[4]. In **Fig. 2**, it is found that, under the same parameters (m, β, S, F, Θ), an unstable region ($\mathrm{Re}[\lambda_0] > 0$) in the present study is larger than that in the previous study. The critical aspect ratio β_c (the minimum aspect ratio that the flat bed is unstable and evolves into the fluvial bars) becomes lower in the present study comparing with the previous study (from $\beta_c = 10.5$ to $\beta_c = 8.2$). Kovacs and Parker's formula[9] tends to underestimate the effect of local slope in the lateral direction while the new bed load formula by Parker *et al.*[8] takes into account of the effect appropriately. Therefore, the flat bed is stabilized particularly in the range of large wave numbers. In the next sections, the comparisons between the experimental results[6),10)–14)] and the present and previous analyses will be provided.

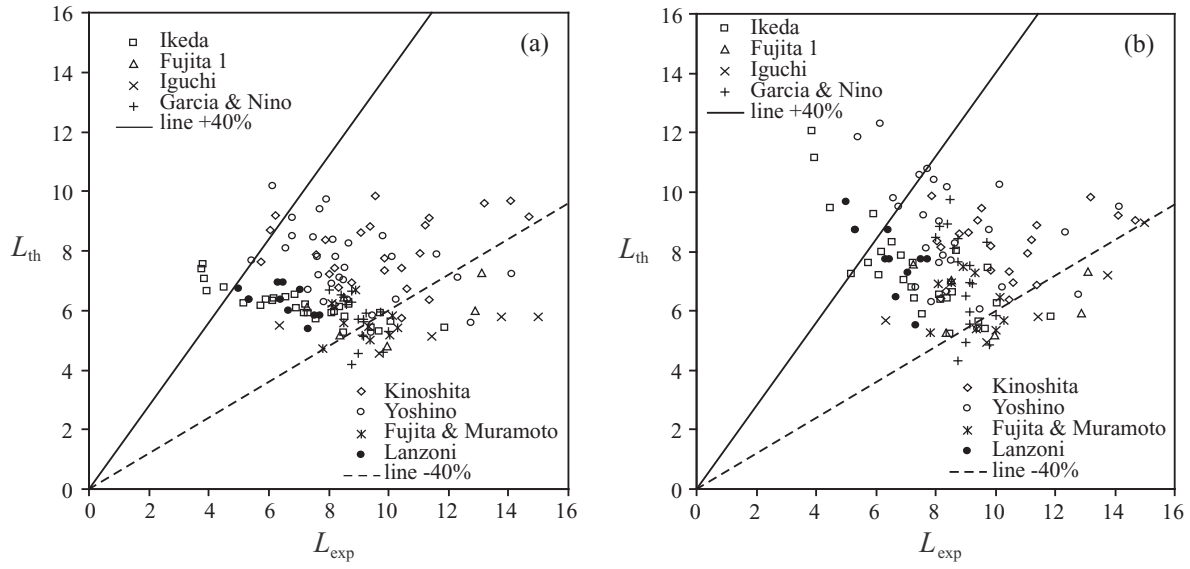

Fig. 3 Comparison of the normalized alternate bar length between the theory and the experiments, where (a) is the present analysis, and (b) is the previous analysis.

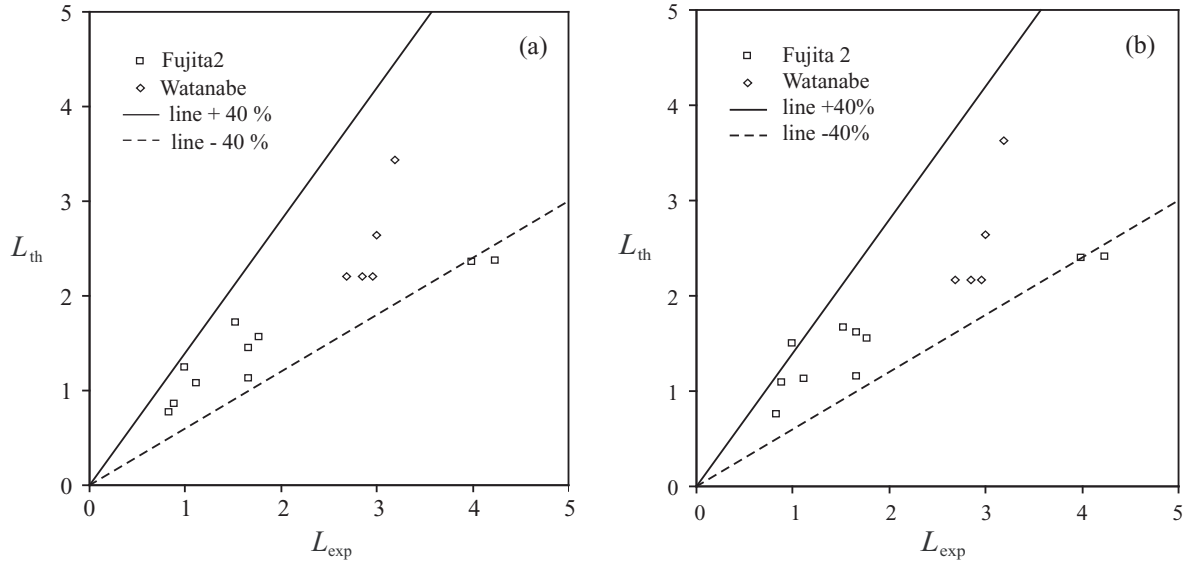

Fig. 4 Comparison of the normalized multiply bar length between the theory and the experiments, where (a) is the present analysis, and (b) is the previous analysis.

3.1 Fluvial bar length

The total of 158 experimental cases provide fluvial bar lengths $\tilde{L}_{\rm exp}$. While the previous analysis can estimate $\tilde{L}_{\rm th}$ for 138 cases out of total 158 cases, the present study can estimate $\tilde{L}_{\rm th}$ for a higher number of 147 cases. As discussed in the previous section, the new bed load formula provides a lower value of the critical aspect ratio β_c. Thus, some cases, where the aspect ratios β are low and the previous study cannot predict $\tilde{L}_{\rm th}$, are found to be able to be estimated by the present study. The comparisons of the normalized alternate and multiple bar lengths L between the experiments and the analyses are shown in **Figs. 3** and **4**, respectively. The normalized experimental bar length $L_{\rm exp}$ and the normalized theoretical bar length $L_{\rm th}$ are

$$L_{\rm exp} = \frac{\tilde{L}_{\rm exp}}{W}, \quad L_{\rm th} = \frac{2\pi}{k_{\rm max}} \qquad (25a, b)$$

where $k_{\rm max}$ is the wave number corresponding to the maximum linear growth rate Re$[\lambda_0]$.

For the quantitative evaluation of two analyses, the following two indices, the mean discrepancy ratio M_D and the mean absolute discrepancy ratio M_A, are in-

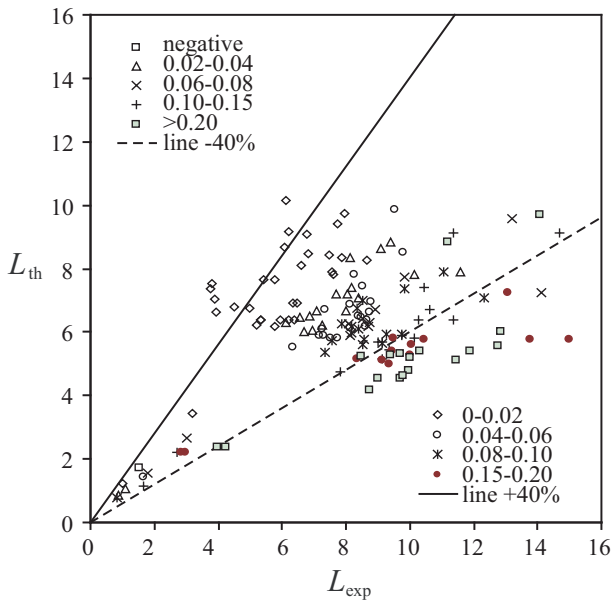

Fig. 5 Comparison of the normalized bar length between the present theory and the experiments, where the legend shows the equilibrium amplitude squared A_e^2.

troduced:

$$M_D = \frac{1}{N}\sum_{i=1}^{N}\frac{L_{\mathrm{th},i} - L_{\mathrm{exp},i}}{L_{\mathrm{exp},i}} \tag{26a}$$

$$M_A = \frac{1}{N}\sum_{i=1}^{N}\left|\frac{L_{\mathrm{th},i} - L_{\mathrm{exp},i}}{L_{\mathrm{exp},i}}\right| \tag{26b}$$

where N is the total number of data. While M_D and M_A take values of -0.16 and 0.29, respectively, for the present study, M_D and M_A take values of -0.06 and 0.30, respectively, for the previous study. However, if the same number of data ($N = 138$ in both analyses) are used, M_D and M_A of the present study become -0.19 and 0.28, respectively.

The indices M_D and M_A represent the bias and the accuracy of the analyses, respectively. It is found that the accuracy of the present analysis using the new bed load formula (**Figs. 3a** and **4a**) is better than the previous study (**Figs. 3b** and **4b**). However, the present analysis underestimates the bar lengths comparing with the previous analysis.

According to Fujita and Muramoto[11], initial bar lengths are found to increase as fluvial bars develop. For example, in their run H-2, the initial alternate bar length is around 2 m. However, the bar length becomes almost 5 m when it is fully developed. Since bar length estimated by our analysis is computed by the wave number $k_{\max}$ corresponding to the maximum linear growth rate in (25b), the discrepancy of bar length may be due to the nonlinear interactions. In **Fig. 5**, the comparison of the normalized bar length between the experiments and the present analysis is re-plotted according to the equilibrium amplitude squared A_e^2. It is found that the equilibrium amplitude A_e affects the estimation of bar lengths significantly. If A_e is large, bar lengths are found to be underestimated. Therefore, it implies that bar length increases considerably by the nonlinearity when A_e is large.

3.2 Fluvial bar celerity

The normalized experimental bar celerity $C_{b\,\mathrm{exp}}$ and the normalized theoretical bar celerity $C_{b\,\mathrm{th}}$ are

$$C_{b\,\mathrm{exp}} = \frac{(1-\lambda_p)H_n\tilde{C}_{b\mathrm{exp}}}{Q_n} \tag{27a}$$

$$C_{b\,\mathrm{th}} = \frac{\mathrm{Im}[\lambda_0] + A_e^2\mathrm{Im}[\lambda_1]}{k_{\mathrm{exp}}} \tag{27a}$$

In **Fig. 6**, it is found that both present and previous studies overestimate bar celerity greatly. However, the present study provides better agreement with the experimental bar celerity than the previous study. Lanzoni[14] performed a linear stability analysis and found that his linear analysis also overestimate bar celerity significantly. He suggested that the nonlinear interactions may influence appreciably bar celerity. However, our analyses show that the agreement does not improve satisfactorily, even though the nonlinear interactions are included in (27b). Recently, Francalanci *et al.*[15] performed numerical simulations to investigate bar formation using the nonlinear and linearized versions of bed load formulae by Parker *et al.*[8]. They found that, using the nonlinear version of bed load formula, bar celerity is smaller than that using the linearized version. Thus, we hypothesize that the estimation of bed celerity may be improved if the nonlinear version of the bar load formula by Parker *et al.*[8] is employed.

4. Conclusion

The weakly nonlinear stability analysis of fluvial bars using the linearized version of the new bed load formula by Parker *et al.*[8] is performed. From the results of the present analysis, better agreements on bar length and bar celerity with the experimental data are found when comparing with the previous analysis[4] using bed load formula by Kovacs and Parker[9]. However, the present analysis still overestimates bar celerity considerably. Since bar formation is strongly influenced by steep transverse bed slopes, it is possible that using the linearized version of the new bed load formula is maybe not good enough to predict bar celerity. Thus, the nonlinear version of the new bed load formula will be employed in the future.

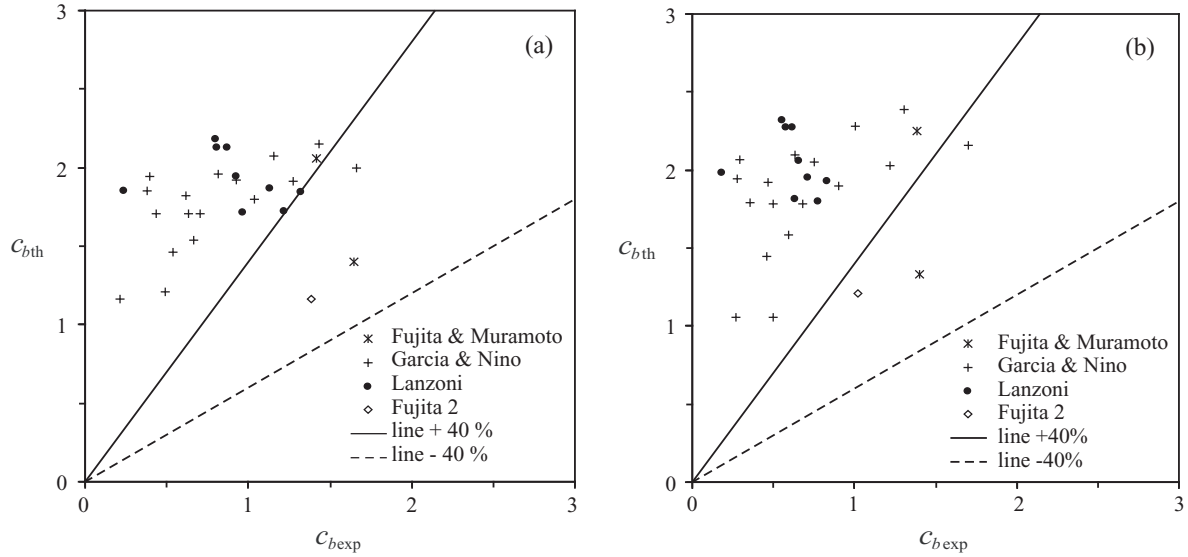

Fig. 6 Comparison of the normalized bar celerity between the theory and the experiments, where (a) is the present analysis, and (b) is the previous analysis.

Acknowledgement: This work was supported by the Hokkaido River Disaster Prevention Research Center and the Japan Society for the Promotion of Science Postdoctoral Fellowship Program (grant-in-aid P 07116).

REFERENCES

1) Fukuoka, S. and Yamasaka, M.: Equilibrium height of alternate bars based on non-linear relationships among bed profile, flow and sediment discharge, *Proc. of JSCE*, Vol. 357/II–3, pp.45–54, 1985. (in Japanese)
2) Colombini, M., Seminara, G. and Tubino, M.: Finite amplitude alternate bars, *J. Fluid Mech.*, Vol. 181, pp.213–232, 1987.
3) Schielen, R., Doelman, A. and de Swart, H. E.: On the nonlinear dynamics of free bars in straight channels, *J. Fluid Mech.*, Vol. 252, pp.325–356, 1993.
4) Izumi, N. and Pornprommin, A.: Weakly nonlinear analysis of bars with the use of the amplitude expansion method, *J. Hyd., Coastal and Env. Eng.*, No. 712/II-60, JSCE, pp.73–86, 2002. (in Japanese)
5) Pornprommin, A., Izumi, N. and Tsujimoto, T.: Weakly nonlinear analysis of multimodal fluvial bars, *Ann. J. Hyd. Eng.* 48, JSCE, pp.1009–1014, 2004.
6) Watanabe, Y.: A weakly nonlinear analysis of bar mode reduction process, *J. Hydroscience & Hydraulic Eng.* 25(1), JSCE, pp.107–122, 2007.
7) Seminara, G., Solari, L. and Parker, G.: Bed load at low Shield stress on arbitrarily sloping beds: Failure of the Bagnold hypothesis, *Water Resour. Res.* 38(11), 1249, doi:10.1029/2001WR000681, 2002.
8) Parker, G., Seminara, G. and Solari, L.: Bed load at low Shield stress on arbitrarily sloping beds: Alternative entrainment formulation, *Water Resour. Res.* 39(7), 1183, doi:10.1029/2001WR001253, 2003.
9) Kovacs, A. and Parker, G.: A new vectorial bedload formulation and its application to the time evolution of straight channels, *J. Fluid Mech.*, Vol.267, pp.153–183, 1994.
10) Ikeda, S.: Prediction of alternate bar wavelength and height, *J. Hydraul. Eng.*, 110(4), pp.371–386, 1984.
11) Fujita, Y. and Muramoto, Y.: Stuies on the process of development of alternate bars, *Bull. Disaster Prev. Res. Inst. Kyoto Univ.*, 35, (Part 3, 314), pp.55–86, 1985.
12) Fujita, Y.: Bar and channel formation in braided streams, in *River Meandering*, edited by S. Ikeda and G. Parker, Water Resour. Mono., AGU, pp.500–560, 1989.
13) Garcia, M. H. and Nino, Y.: Dynamics of sediment bars in straight and meandering channels: Experiments on the resonance phenomenon, *J. Hydraul. Res.*, 31, pp.739–761, 1993.
14) Lanzoni, S.: Experiments on bar formation in a straight flume 1. Uniform sediment, *Water Resour. Res.* 36(11), pp.3337–3349, 2000.
15) Francalanci, S., Solari, L. and Toffolon, M.: Local high-slope effects on sediment transport and fluvial bed form dynamics, *Water Resour. Res.* 45, W05426, doi:10.1029/2008WR007290, 2009.

(Received March 9, 2010)